3(a) for selected couples of emissivities. If we consider now the reversal [Table 3(b)], the maximum velocities can be obtained either near the cold wall or near the hot wall according to the values of the difference $(\varepsilon_1 - \varepsilon_2)$. The dominant wave then moves upward or downward. Therefore, the behavior of the flow *vis-à-vis* the disturbances cannot be predicted unlike when using the linear approximation.

The results of the stability analysis were complemented by some numerical simulations in order to have other information about the structure of the flow. There again, the computations are in agreement with the theoretical findings regarding both the stabilizing effect shown in Table 2 and the motion of the cells depicted previously (critical wave numbers and wave speeds). What is learnt from the simulations in a slot of finite aspect ratio is that the instability develops locally: from the streamline patterns plotted for one of the extreme cases ($\varepsilon_1 = 0, \varepsilon_2 = 1$), the cells are seen in the lower half part of the cavity and for the other ($\varepsilon_1 = 1, \varepsilon_2 = 0$), the cells are in the upper part. These patterns show that the dominant travelling wave fills the end of the cavity. However, as seen from the distribution of the stream function in the central middle plane, the cells due to this kind of dissymmetry are weak at the onset of instability (variations of the streamfunction within 5% at $Gr = 16\,000$ for the case shown in Table 2). Finally the analogy between the present results and those obtained in a fluid contained in a vertical annulus [11, 12] must be emphasized again. Since streamlines patterns are not shown in this paper due to space limitation, the reader could find similar pictures of the effects of a reflecting hot wall by referring to the paper of Lee *et al.* [11] in which the inner cylinder is hot. The case of a reflecting cold wall corresponds to an outer hot cylinder.

CONCLUSION

Linear stability theory is used to study the conditions marking the onset of convective instabilities in vertical layers of radiating fluids. The calculations are done without linearizing the radiation term in the base flow equations and for dissimilar radiative boundary conditions. In the conduction and transition regimes, the results show that the instabilities set in as a single travelling wave whose moving direction is strongly dependent on the emissivities of the bounding walls. For higher stratification parameters, one of the two oppositely travelling waves which are seen for symmetric base flows dies out. The multicellular structures of flows obtained by numerical integration of the equation governing the motion in a slender cavity are found to be in agreement with the predictions of the stability theory.

REFERENCES

1. G. Desrayaud and G. Lauriat, On the stability of natural convection of a radiating fluid in a vertical slot, *Int. Commun. Heat Mass Transfer* **11**, 439–450 (1984).
2. V. S. Arpaci and Y. Bayazitoglu, Thermal stability of radiating fluids: asymmetric slot problem, *Phys. Fluids* **16**, 589–593 (1973).
3. M. A. Hassab and M. N. Özişik, Effects of radiation and convective boundary conditions on the stability of fluid in an inclined slender slot, *Int. J. Heat Mass Transfer* **22**, 1095–1105 (1979).
4. R. F. Bergholz, Instability of steady natural convection in a vertical fluid layer, *J. Fluid Mech.* **84**, 743–768 (1978).
5. V. S. Arpaci and D. Gözüm, Thermal instability of radiating fluids: the Bénard problem, *Phys. Fluids* **16**, 581–588 (1973).
6. A. M. Shaaban and M. N. Özişik, The effect of nonlinear density stratification on the stability of a vertical water layer in the conduction regime, *Trans. Am. Soc. mech. Engrs, J. Heat Transfer* **105**, 130–137 (1983).
7. A. M. Shaaban and M. N. Özişik, Effect of curvature on the thermal stability of a fluid between two vertical coaxial cylinders, *Proc. 7th Int. Conference Heat and Mass Transfer*, Vol. 2, NC 27, pp. 281–286 (1982).
8. C. M. Vest and V. S. Arpaci, Stability of natural convection in a vertical slot, *J. Fluid Mech.* **36**, 1–16 (1969).
9. G. Desrayaud and G. Lauriat, Natural convection of a radiating fluid in a vertical layer, *J. Heat Transfer* (in press).
10. G. Lauriat, Combined radiation–convection in gray fluids enclosed in vertical cavities, *J. Heat Transfer* **104**, 609–615 (1982).
11. Y. Lee, S. A. Korpela and R. N. Horne, Structure of multicellular natural convection in tall vertical annulus, *Proc. 7th Int. Conference Heat and Mass Transfer*, Vol. 2, NC 17, pp. 221–226 (1982).
12. I. G. Choi and S. A. Korpela, Stability of the conduction regime of natural convection in a tall vertical annulus, *J. Fluid Mech.* **99**, 725–738 (1980).

Int. J. Heat Mass Transfer. Vol. 28, No. 8, pp. 1617–1621, 1985
Printed in Great Britain

0017-9310/85 $3.00 + 0.00

Parameterization of system behavior for salt-stratified solutions heated from below with and without salinity-maintained mixed layers

T. L. BERGMAN, F. P. INCROPERA and R. VISKANTA

Heat Transfer Laboratory, School of Mechanical Engineering, Purdue University, West Lafayette, IN 47907, U.S.A.

NOMENCLATURE

C	constant
c_v	specific heat
g	gravitational acceleration
k	thermal conductivity
L	arbitrary length
m_s	salt mass fraction
q_b	applied bottom heat flux
Ra_s^*	solutal Rayleigh number, $g\beta_s(dm_s/dz)_i L^4/\alpha\nu$
Ra_T^*	modified thermal Rayleigh number, $g\beta_T q_b L^4/k\alpha\nu$
T	temperature
t	time
X	ratio of modified thermal Rayleigh number to solutal Rayleigh number
Y	dimensionless parameter, $(dm_s/dz)_i(X\alpha t)^{1/2}/m_{s,o}$
z	vertical space coordinate positive upward.

Greek symbols

α	thermal diffusivity, $k/(\rho c_v)$
β_s	solutal expansion coefficient, $\rho^{-1}\,\partial\rho/\partial m_s\|_T$
β_T	thermal expansion coefficient, $\rho^{-1}\,\partial\rho/\partial T\|_{m_s}$

Δm_s salinity difference across the interfacial boundary layer
δ_b mixed layer height
δ_p thermal penetration height
ν kinetic viscosity
ρ mass density
θ dimensionless temperature.

Subscripts
b bottom
d diffusive region
i initial
m maintained
o initial condition at $z = 0$
u unmaintained.

INTEREST in engineering applications of double-diffusive convection has stimulated the development of mathematical models for predicting the response of an initially isothermal, salt-stratified fluid to destabilization by an applied bottom heat flux [1, 2]. Local thermal instabilities induce convective motion in a mixed layer which gradually expands at the expense of an overlying stable region, as fluid is entrained through a thin interfacial boundary layer separating the two regions. As the mixed layer expands, it warms and serves as a heat source for the stable region, which is characterized by an upward propagating temperature profile. The rate of growth of the mixed layer decreases with time, as the stabilizing salinity difference across the interfacial boundary layer increases with increasing mixed layer height. Since the salinity distribution limits mixed layer growth, it has been suggested [3] that system behavior may be modified by controlling the salinity, as, for example, by maintaining a fixed mixed layer salinity.

A schematic of typical temperature, salinity, and density distributions is shown in Fig. 1. Salinity and density distributions are shown for maintained (the mixed layer salinity is maintained at the maximum value, $m_{s,o}$) and unmaintained conditions.

Although models have been developed to predict the transient behavior of a thermally destabilized, salt-stratified system, little has been done to determine relevant dimensionless parameters. In addition, although means to alter system behavior by controlling the mixed layer salinity have been suggested, the effects of such control have not been studied. As such, an objective of this study has been to use an accepted multi-layer model of system behavior [1] to infer the form of dimensionless parameters which govern mixed layer height, salinity and temperature and to predict system response in terms of the parameters for salt maintained and unmaintained conditions.

A model of system behavior has been developed by applying energy and species balances to control volumes about the bottom mixed layer of height δ_b and the portion of the stable region affected by the upward propagating temperature profile of penetration height δ_p [1]. The integrated form of the heat equation is applied to the stable region, and an additional input to the model is an empirical correlation for the mixed layer growth rate, $d\delta_b/dt$. Species diffusion in the stable region is neglected, while the stabilizing density difference across the interfacial boundary layer is assumed to be due solely to the salinity difference. Predictions of mixed layer height, salinity, and temperature have been experimentally verified over a broad range of experimental conditions.

The model equations include the following coupled differential equations [1],

$$\frac{d\delta_b}{dt} = \frac{0.20\beta_T q_b}{c_{v,b}\Delta m_s \rho \beta_s} \tag{1}$$

$$\frac{dT_b}{dt} = \frac{q_b + 2k_b(T_i - T_b)/(\delta_p - \delta_b)}{\rho_b c_{v,b}\delta_b} \tag{2}$$

$$\frac{d\delta_p}{dt} = \frac{\dfrac{-6\alpha_d(T_i - T_b)}{(\delta_p - \delta_b)} - \dfrac{dT_b}{dt}(\delta_p - \delta_b) - 2\dfrac{d\delta_b}{dt}(T_b - T_i)}{(T_b - T_i)} \tag{3}$$

for the mixed layer height and temperature and the thermal penetration depth, as well as an expression for the salinity difference across the interfacial boundary layer. The salinity difference $\Delta m_s = m_{s,b} - m_s(z = \delta_b)$ is

$$\Delta m_s = [m_{s,o} + (dm_s/dz)_i \delta_b/2] - m_s \quad (z = \delta_b) \tag{4}$$

or

$$\Delta m_s = m_{s,o} - m_s \quad (z = \delta_b) \tag{5}$$

for unmaintained and maintained conditions, respectively. Thermophysical properties may be evaluated from tabulated data for saline water [4].

Assuming constant properties, equation (4) or (5) may be substituted into equation (1) which may be integrated and expressed in the dimensionless forms

$$\frac{\delta_b}{(t\alpha)^{1/2}} = CX^{1/2} \tag{6}$$

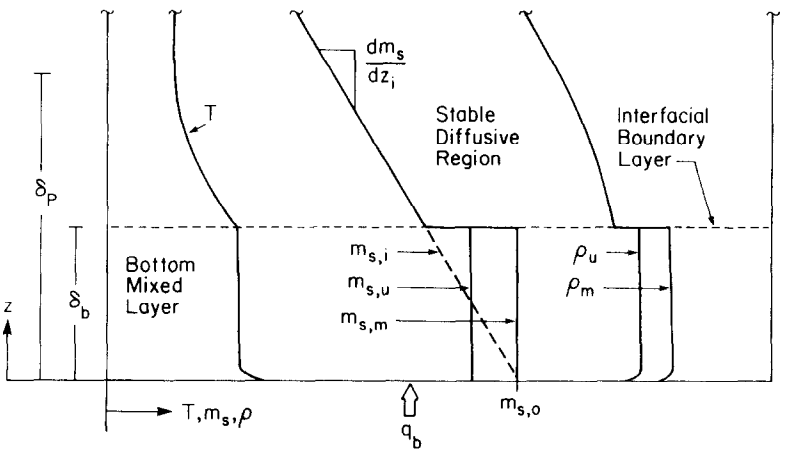

FIG. 1. Schematic of a thermally destabilized salt-stratified system.

where $C = 0.894$ or 0.632 for the unmaintained and maintained cases, respectively. The ratio of the modified thermal to solutal Rayleigh number,

$$X \equiv \frac{Ra_T^*}{Ra_s^*} = \frac{\beta_T q_b}{k\beta_s(dm_s/dz)_i} \tag{7}$$

determines the relative influence of the destabilizing temperature and stabilizing salinity gradients.

The dimensionless mixed layer salinity for the unmaintained system may be determined by substituting equation (6) into the first term on the RHS of equation (4) to yield

$$\frac{m_{s,b}}{m_{s,o}} = 1 + 0.447Y \tag{8}$$

where the dimensionless parameter

$$Y \equiv \frac{(dm_s/dz)_i(X\alpha t)^{1/2}}{m_{s,o}} \tag{9}$$

may be interpreted as the ratio of the mixed layer salinity reduction due to expansion of the mixed layer into a region of lower salinity to the initial salinity at $z = 0$.

If heat transfer from the bottom mixed layer to the stable region and property variations are neglected, equations (2) and (6) yield a constant dimensionless bottom mixed layer temperature of the form

$$\theta \equiv \frac{(T_b - T_i)(Xk\rho c_v)^{1/2}}{q_b t^{1/2}} = C \tag{10}$$

where $C = 1.12$ or 1.58 for the unmaintained and maintained cases, respectively.

To investigate system behavior, calculations based on equations (6), (8) and (10) are compared with detailed numerical simulations for nine conditions. Values of $(dm_s/dz)_i$, q_b and X (calculated using thermophysical properties evaluated at $T_i = 20°C$ and $m_{s,o} = 25‰$) for each condition are shown in Table 1.

Table 1. Conditions associated with the numerical simulations

Simulation	$dm_s/dz\|_i$ (‰ m^{-1})	q_b (W m^{-2})	X
1	2.5	100	2.061
2	2.5	200	4.121
3	2.5	400	8.242
4	5.0	100	1.030
5	5.0	200	2.061
6	5.0	400	4.121
7	10.0	100	0.515
8	10.0	200	1.030
9	10.0	400	2.061

Dimensional mixed layer heights, salinities, and temperatures are shown in Figs. 2–4. As shown in Fig. 2, mixed layer growth rates increase with increasing X, and growth of a salinity-maintained mixed layer is slower than that of an unmaintained layer. Apart from the slight variation in δ_b for simulations characterized by the same value of X, the results suggest that X is an appropriate dimensionless parameter to describe layer growth. With fixed X, the variation of mixed layer height is one of increasing δ_b with increasing q_b. As such, the variation of δ_b for a given value of X may be attributed to the variation of thermophysical properties (especially increasing values of β_T) with increased mixed layer temperatures. The constant property solution, given by equation (6) represents the limiting case of minimum predicted mixed layer heights.

Figure 3 shows predicted values of the mixed layer salinity, and results for the unmaintained condition are well correlated by the Y parameter. Due to the underprediction of mixed layer heights (Fig. 2), the constant property solution [equation (8)] overpredicts the results of the numerical simulations. Again, the constant property solution given by equation (8) may be

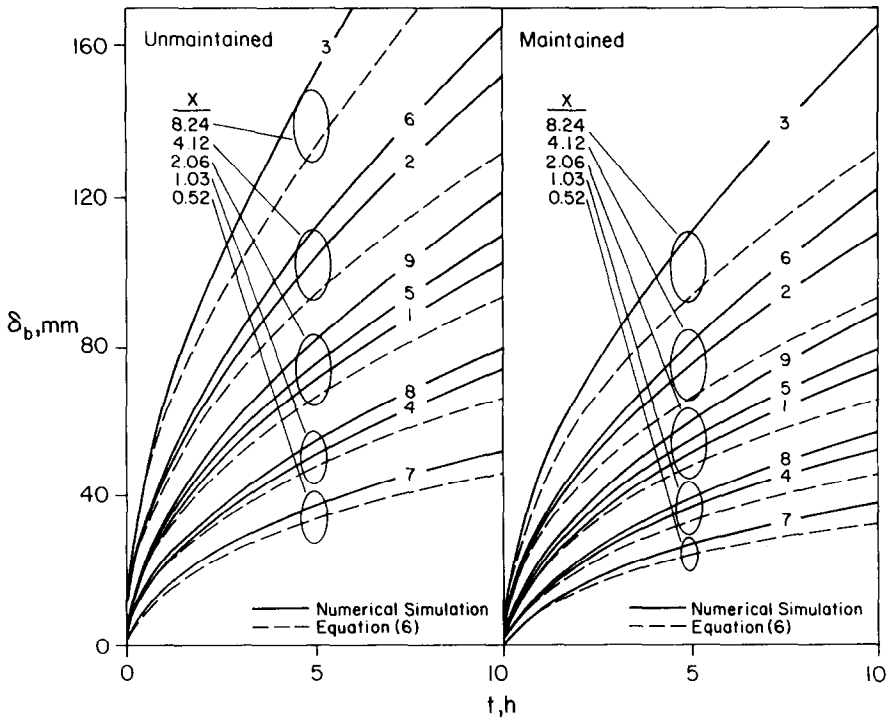

FIG. 2. Mixed layer heights for unmaintained and salinity-maintained systems.

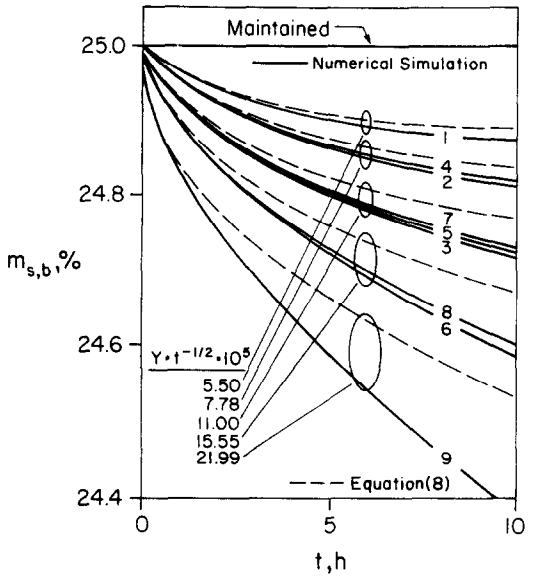

FIG. 3. Mixed layer salinities for unmaintained and salinity-maintained systems.

considered as the limiting case of maximum mixed layer salinities.

Predicted mixed layer temperatures are presented in Fig. 4. Since mixed layer heights decrease with salinity maintenance, there is a corresponding increase in temperature. Also shown in Fig. 4 are selected mixed layer temperatures predicted from equation (10). Clearly, predictions based on equation (10) are much greater than those obtained from the model. This poor agreement may be traced to neglecting heat transfer from the mixed layer to the stable region in developing equation (10). This assumption has been shown to be reasonable for systems characterized by mixed layer growth rates which are comparable to the upward propagation rate of the thermal penetration depth (large X) [5, 6]. Model results suggest that mixed layer temperatures may be predicted to within 20% accuracy using equation (10) for values of X greater than 10.

It would be useful to have expressions relating mixed layer characteristics of salinity-maintained and unmaintained systems. In terms of mixed layer heights, such a relation is obtained from equation (6) which yields $\delta_{b,u}/\delta_{b,m} = 1.41$ for systems with identical values of X and α. Values of the ratio predicted by the complete model, which accounts for variable properties, are 1.38 ± 0.02.

Since mixed layer temperatures were poorly described by equation (10), it may be unreasonable to expect a correlation between unmaintained and maintained mixed layer temperatures. However, results of the numerical simulations indicate that the ratio of reduced mixed layer temperatures, $(T_{b,m} - T_i)/(T_{b,u} - T_i)$, is a function of the Rayleigh number ratio, X. This functional dependence is well represented by the expressions.

$$\frac{T_{b,m} - T_i}{T_{b,u} - T_i} = 1.0786 + 0.11208X - 0.0257X^2$$

$$0.2 \leqslant X < 2.0 \quad (12a)$$

$$\frac{T_{b,m} - T_i}{T_{b,u} - T_i} = 1.1536 + 0.02575X - 0.00127X^2$$

$$2.0 \leqslant X \leqslant 10.0. \quad (12b)$$

In conclusion, it may be said that mixed layer hgiehts and salinities are well correlated by the dimensionless parameters of this study and the correlations may be used in lieu of more complicated models to reliably predict these quantities from knowledge of the initial stratifying salinity gradient and bottom heat flux. Mixed layer temperatures are overpredicted by equation (10) due to assumptions inherent in its development. Reliable relationships for ratios of mixed layer heights, salinities, and temperatures for salinity maintained and unmaintained systems have also been developed.

Acknowledgement—Support of this work by the National Science Foundation under Grant No. MEA-8316580 is gratefully acknowledged.

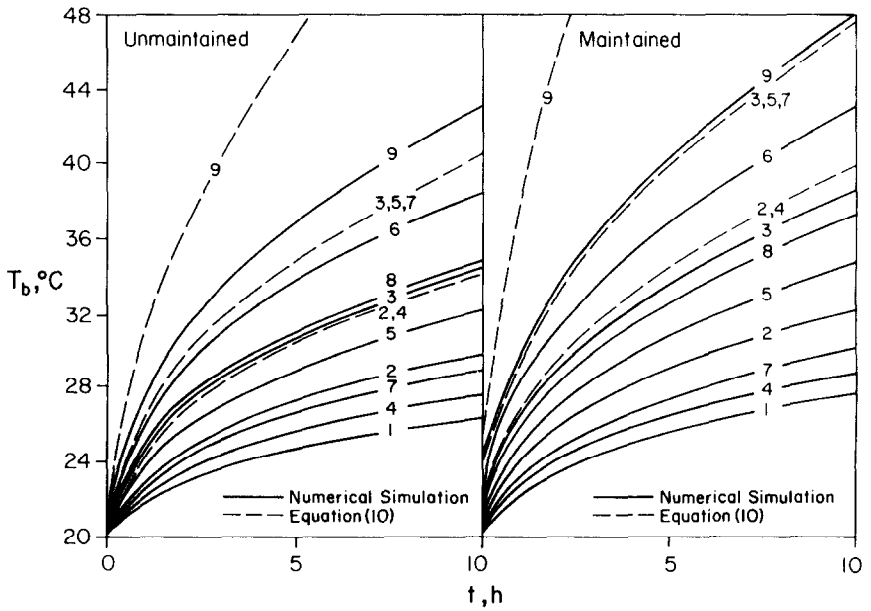

FIG. 4. Mixed layer temperatures for unmaintained and salinity-maintained systems.

REFERENCES

1. T. L. Bergman, F. P. Incropera and R. Viskanta, A multilayer model for mixing layer development in a double-diffusive thermohaline system heated from below, *Int. J. Heat Mass Transfer* **25**, 1411–1418 (1982).
2. T. L. Bergman, F. P. Incropera and R. Viskanta, A differential model for salt-stratified, double-diffusive systems heated from below, *Int. J. Heat Mass Transfer* **28**, 779–788 (1985).
3. C. E. Nielsen, Salt transport and gradient maintenance in solar ponds, *Proc. AS-ISES*, Houston, pp. 179–184 (1982).
4. United States Office of Saline Water, Technical Data Book (1964).
5. J. S. Turner, The behaviour of a stable salinity gradient heated from below, *J. Fluid Mech.* **33**, 183–200 (1968).
6. H. E. Huppert and P. F. Linden, On heating a stable salinity gradient from below, *J. Fluid Mech.* **95**, 431–464 (1979).

Int. J. Heat Mass Transfer. Vol. 28, No. 8, pp. 1621–1624, 1985
Printed in Great Britain

0017-9310/85 $3.00 + 0.00
Pergamon Press Ltd.

Effects of magnetic field and non-uniform temperature gradient on Marangoni convection

N. RUDRAIAH, V. RAMACHANDRAMURTHY
UGC-DSA Centre in Fluid Mechanics, Department of Mathematics, Central College, Bangalore University, Bangalore-560001, India

and

O. P. CHANDNA
Department of Mathematics, University of Windsor, Windsor, Canada N9B 3P4

(*Received December* 1983)

NOMENCLATURE

a	resultant horizontal wave number, $(l^2+m^2)^{1/2}$
d	thickness of the fluid layer
D	d/dz
$f(z)$	a non-dimensional temperature gradient, $-\frac{d}{\Delta T}\frac{dT_0}{dz}$
$\mathbf{H}$	magnetic field
$\hat{\mathbf{k}}$	unit vector in the z-direction
l, m	horizontal wave numbers in the directions of x- and y-axes
M	Marangoni number, $\frac{\sigma_T \Delta T d}{\rho\delta\kappa}$
M_c	critical Marangoni number
Pr	magnetic Prandtl number, δ/δ_m
Pr	Prandtl number, δ/κ
$\mathbf{q}$	velocity, (u, v, w)
Q	Chandrasekhar number, $\frac{\mu H_0^2 d^2}{\rho\delta\delta_m}$
T	temperature
T_0	basic temperature
ΔT	temperature difference between two boundaries
t	time
W	z-component of velocity
(x, y, z)	Cartesian coordinates
∇^2	$\frac{\partial^2}{\partial x^2}+\frac{\partial^2}{\partial y^2}+\frac{\partial^2}{\partial z^2}$.

Greek symbols

α	a^2
κ	thermal diffusivity
μ	magnetic permeability
ν	kinematic viscosity
ν_m	magnetic viscosity
ρ	mass density
σ	electrical conductivity
σ_T	variation of surface tension with temperature
σ_0, σ_1	constants
ε	quasi-time-dependent thermal depth
δ	Dirac's delta-function.

INTRODUCTION

THE MECHANISM of controlling convection generated in a fluid either by the buoyancy force or by the surface tension variation with temperature or by both has recently assumed importance in material processing in space [1] because of its application to the possibility of producing various new materials. The range of possibilities extends from producing large crystals of uniform properties to manufacturing materials with unique properties. The reduced gravity (i.e. microgravity) environment provided during sustained space flight prevents convection generated by the buoyancy force called Rayleigh–Bénard convection. But the other type of convection generated by variation of surface tension with temperature [2, 3] called Marangoni convection [4], can still exist. Such convection may also influence the local material composition and the shape of the solid–liquid interface. This can result in materials with non-uniform properties and crystal defects. Forces like Lorentz force due to electromagnetic effects [5, 6], coriolis force due to rotation [7] and non-uniform temperature gradient due to transient heating or cooling [8] at the boundaries, which are ineffective at the terrestrial environment, become effective in the microgravity